Anisotropic CE-type orbital correlations in the ferromagnetic metallic phase of $Nd_{1/2}Sr_{1/2}MnO_3$

J. Geck,[1] D. Bruns,[1] C. Hess,[1] R. Klingeler,[1] P. Reutler,[1] M. v. Zimmermann,[2] S.-W. Cheong,[3] and B. Büchner[1]

[1]*2. Physikalisches Institut/Lehrstuhl A, RWTH Aachen, 52056 Aachen, Germany*
[2]*HASYLAB at DESY, Notkestr. 85, 22065 Hamburg, Germany*
[3]*Department of Physics and Astronomy, Rutgers University, Piscataway, New Jersey 08854*

We present hard x-ray scattering studies of the charge and orbital ordering in $Nd_{1/2}Sr_{1/2}MnO_3$ together with magnetization and thermal expansion measurements as a function of temperature and magnetic field. Superstructure reflections corresponding to the orbital ordering below $T_{CO} \simeq 160$ K are observed in the ferromagnetic metallic phase up to 200 K. The correlation length of the observed structural modulations is found to be highly anisotropic; i.e., the correlations exist predominantly in the ab planes. Moreover, the periodicity of the superstructure modulations is the same above and below T_{CO}. As a consequence, the modulations found in the ferromagnetic metallic phase are incommensurate to the average lattice structure. The results from hard x-ray scattering, thermal expansion, and magnetization studies can be consistently interpreted in terms of short-range orbital ordering in the ferromagnetic metallic phase of $Nd_{1/2}Sr_{1/2}MnO_3$.

I. INTRODUCTION

The doped manganites are fascinating examples of materials with strongly correlated electrons exhibiting a great variety of intriguing phenomena. Their unusual physical properties originate from the intimate coupling between electronic, structural, magnetic, and orbital degrees of freedom[1-3] which has been recently observed and intensively discussed. A very interesting example for the simultaneous ordering of magnetic, charge, and orbital degrees of freedom is the insulating ground state of the half-doped perovskite manganites shown in Fig. 1. As a result of strong electronic correlations ferromagnetic charge- and orbital-ordered zigzag chains are formed in the ab planes which are coupled antiferromagnetically to each other, resulting in the so-called antiferromagnetic CE structure.[4] In what follows we will refer to this phase shortly as the CE phase and we call the corresponding ordering of the different degrees of freedom CE-type magnetic, charge, and orbital order, respectively.

This particular type of ordering has been experimentally observed in several half-doped perovskite manganites like $Pr_{1/2}Sr_{1/2}MnO_3$,[5] $Pr_{1/2}Ca_{1/2}MnO_3$,[6] $La_{1/2}Ca_{1/2}MnO_3$,[7] $Nd_{1/2}Sr_{1/2}MnO_3$,[8,9] and also in the layered compound $La_{1/2}Sr_{3/2}MnO_4$.[10] However, the CE phase of $Nd_{1-x}Sr_xMnO_3$ is only stable at low temperatures in the very narrow doping range $0.48 < x < 0.51$.[11] More specifically, already at $x = 0.45$ the system is a ferromagnetic metal (FMM) at low temperatures whereas at $x = 0.51$ an A-type antiferromagnetic metallic (AFM) ground state is formed. The drastic doping dependence of the ground state around $x = 0.5$ can be understood as follows: In the CE phase a gap opens at the Fermi level and similar to the lattice Peierls effect the electronic energy at half band filling is reduced.[12] Therefore, it is clear that deviations from half filling lead to a destabilization of the CE phase. Furthermore, it is known from band structure calculations that the energy difference between the CE, FMM, and AFM phases is very small (around 0.01

eV/atom).[13] As a consequence, strong fluctuations and in particular phase segregation are to be expected. Indeed, recent x-ray and neutron scattering results reveal the coexistence of the AFM, FMM, and CE phases in $Nd_{1/2}Sr_{1/2}MnO_3$ over a large temperature range.[14-17] As phase segregation might be of crucial importance for the colossal magnetoresistance effect (CMR effect) observed in manganites[18,19] its investigation is not only of interest from a fundamental point of view, but may also be important for possible applications. Another interesting question concerns the origin of the CE phase. While the microscopic structure of this phase has been well established, the mechanism of the ordering phenomena itself is still the subject of controversial discussions.[20,21,12]

In this paper we report hard x-ray scattering studies of short-range orbital correlations in $Nd_{1/2}Sr_{1/2}MnO_3$ above T_{CO} along with measurements of the thermal expansion and magnetization as a function of temperature and magnetic
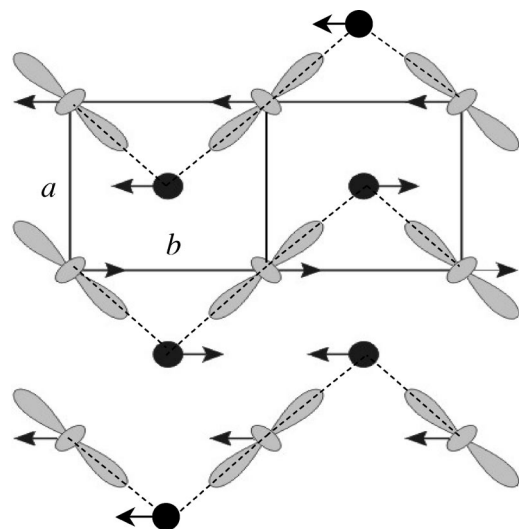

FIG. 1. View of the ab plane in the magnetic, charge, and orbital ordered ground state of $R_{1/2}A_{1/2}MnO_3$ (solid circles, Mn^{4+}; grey lobes, Mn^{3+}). The ab plane consists of ferromagnetic zigzag chains which are antiferromagnetically coupled to each other.

field. We observe $(h,k\pm0.5,0)$ superstructure reflections (throughout this paper all reflections are indexed in the orthorhombic *Pbnm* setting) characteristic for CE-type orbital order in the FMM phase up to 200 K. These correlations start to develop predominantly in the *ab* plane ($\xi_{ab} \simeq 500$ Å) while the orbital order between successive *ab* planes is only weakly correlated ($\xi_{ab}\simeq80$ Å). Moreover, the observed structural modulations are incommensurate with the mean lattice structure of the ferromagnetic metallic phase having the periodicity of the low-temperature phase. Therefore, our results lead to the conclusion that large CE-type orbital-ordered areas persist in the FMM phase of $Nd_{1/2}Sr_{1/2}MnO_3$. Furthermore, the field-dependent measurements show that these CE-type orbital-ordered areas are strongly influenced by applied magnetic fields.

II. EXPERIMENTAL TECHNIQUES

The $Nd_{1/2}Sr_{1/2}MnO_3$ single crystals were grown using the traveling floating zone method and characterized by magnetization, resistivity, and x-ray powder diffraction. The lattice constants as well as the observed macroscopic properties agree well with measurements reported in literature.[11,14] The magnetization measurements have been performed using a vibrating sample magnetometer described elsewhere.[22] For the thermal expansion measurement a capacitance dilatometer was utilized which allows a very accurate study of crystal length changes.[23] Hard x-ray scattering experiments were performed at the beamline BW5 at the HASYLAB in Hamburg using hard x rays with photon energies of 120 keV. Due to the high penetration depths at this energy (~ 1 mm), surface effects have only a minor influence on the detected signal. Therefore, this radiation allows us to investigate the bulk properties of the sample.

We performed triple-axis diffraction in horizontal Laue geometry utilizing the (111) reflection of a Si/Ge-monochromator and Si/Ge-analyzer crystal with mosaicities of 60″. With this setup and the sample used the longitudinal resolution was 0.009 Å^{-1} [full width at half maximum (FWHM)] and the transversal resolution was 0.015 Å^{-1} (FWHM) at the orthorhombic (220) position. The signal was detected by a solid-state Ge detector with a resolution of 500 eV at 100 keV allowing electronical suppression of higher harmonics in the beam. For temperature-dependent measurements between 8 K and 300 K the sample was mounted on the coldfinger of a closed-cycle cryostat which itself was fixed on a standard Huber Eulerian cradle. The measurements in magnetic fields up to 4 T were carried out utilizing a liquid helium cryostat equipped with a superconducting magnet.

III. EFFECTS OF TWINNING

In this study we are mainly concerned with superstructure reflections around the (220) Bragg peak. However, as the investigated samples were twinned in all three directions of the underlying cubic perovskite, the $\langle110\rangle$ direction of one type of twin domains coincides with the $\langle001\rangle$ direction of another type of domain. Therefore, the (2 ± 20) and (004)
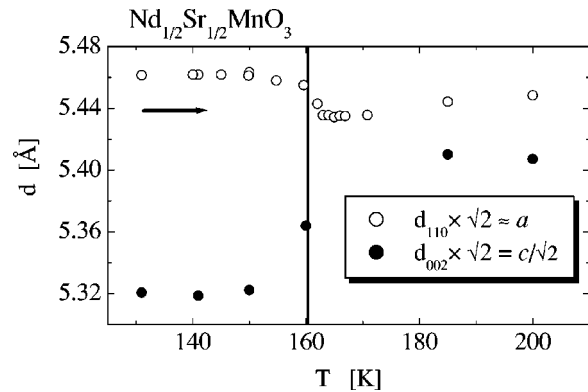

FIG. 2. Temperature dependence of the lattice plane spacings d_{110} and d_{002} as deduced from 2Θ. Explanations are given in the text.

reflections are observed around the same position, having slightly different scattering angles 2Θ. As the *c* parameter is elongated while the *a* and *b* parameters are shortened at T_{CO} upon heating it is possible to discriminate between (2 ± 20) and (004) reflections.

Figure 2 displays the lattice spacings derived from the temperature dependence of the two observed scattering angles 2Θ. Both curves show a clear anomaly at T_{CO}: Upon heating the upper curve decreases at T_{CO} as expected for the (110) lattice plane spacing and the lower curve increases corresponding to the (002) planes. Moreover, the derived lattice spacings are in good agreement with the ones reported in literature.[11]

The results given above show that contributions of $\langle110\rangle$- as well as $\langle001\rangle$-oriented domains have to be taken into account. In particular, we observe superstructure reflections at $(h,k\pm\frac{1}{2},0)$ and $(h\pm\frac{1}{2},k,0)$ due to $\langle110\rangle$ domains with interchanged *a* and *b* directions. Furthermore, it is important to note that the $\langle001\rangle$-oriented domains do not contribute to the intensity at $(h\pm\frac{1}{2},k,0)$ and $(h,k\pm\frac{1}{2},0)$: For example, the $(2\pm\frac{1}{2},2,0)$ reflection of a $\langle001\rangle$ domain corresponds to the $(\pm\frac{1}{4},\mp\frac{1}{4},-4\pm\frac{1}{2})$ reflection of a $\langle110\rangle$ domain. Thus the superstructure reflections of $\langle110\rangle$ and $\langle001\rangle$ domains emerge at different positions. Therefore we can conclude that a radial scan through a $(h,k\pm\frac{1}{2},0)$ or a $(h\pm\frac{1}{2},k,0)$ reflection probes the orbital correlations in the *ab* plane. Moreover, the *l* direction which is common for all $\langle110\rangle$ domains is well defined.

IV. TEMPERATURE-DEPENDENT MEASUREMENTS

In Fig. 3 temperature dependences of the magnetization, electrical resistivity, and integrated intensity of the (2,3/2,0) superstructure reflection are compared. In the temperature range between 270 K and 4.2 K two phase transitions can be observed. The first transition takes place at $T_C=249.5$ K where the pronounced increase of the magnetization signals the onset of ferromagnetic order. In accordance with the double-exchange model, the electrical resistivity is reduced and shows a metallic characteristic in the temperature range of increased magnetization. Therefore, this phase is often called the ferromagnetic metallic phase, although it has to be
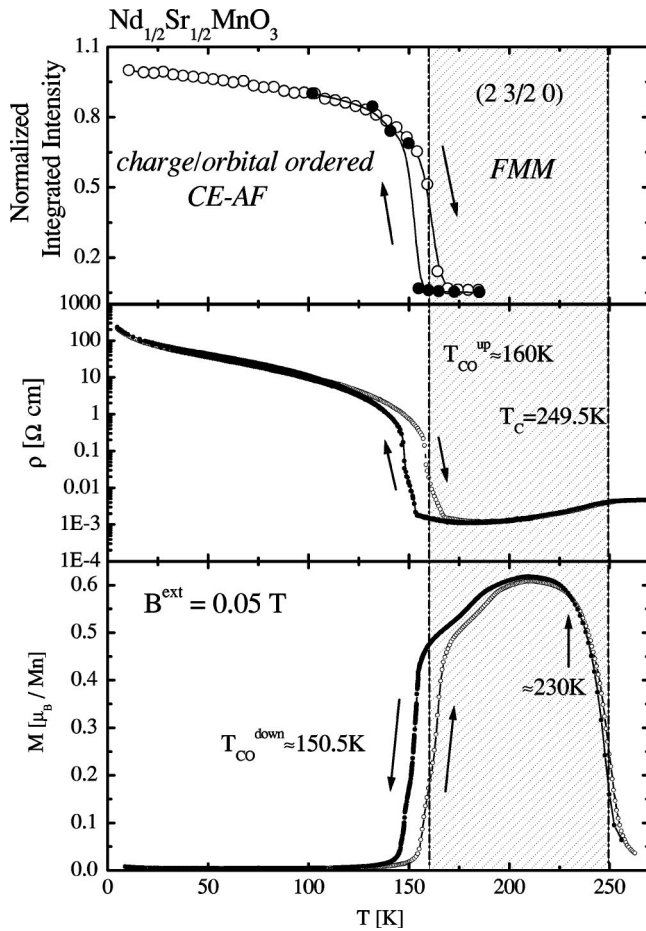
FIG. 3. Top: normalized integrated intensity of the (2,3/2,0) superstructure reflection measured in zero field. Middle: zero-field resistivity of the same sample as a function of temperature on a logarithmic scale. Bottom: magnetization vs temperature in an applied magnetic field of 0.05 T.

noted that the resistivity is still about three orders of magnitude larger than that of a typical metal. The second phase transition takes place at $T_{CO}^{down} \simeq 150.5$ K upon cooling. At this temperature the macroscopic magnetization is strongly reduced and the resistivity increases by about three orders of magnitude. Moreover, the observation of the (2,3/2,0) superstructure reflection signals the doubling of the orthorhombic unit cell. These observations can be attributed to the development of the CE antiferromagnetic, charge- and orbital-ordered ground state (Fig. 1), which has been established by numerous experimental and theoretical investigations. In what follows we will refer to this transition as the CO/OO transition.

Focusing on the CO/OO transition a pronounced temperature hysteresis is observed in all three measurements ($T_{CO}^{up} \simeq 160$ K, $T_{CO}^{down} \simeq 150.5$ K) indicating the first-order character of the transition. In particular, the temperature hysteresis of the resistivity and the integrated intensity at the (2,3/2,0) position correspond nicely to each other, showing that both measurements characterize the same ordering phenomenon. However, the temperature dependence of the magnetization displays a remarkable behavior: First, the temperature hys-
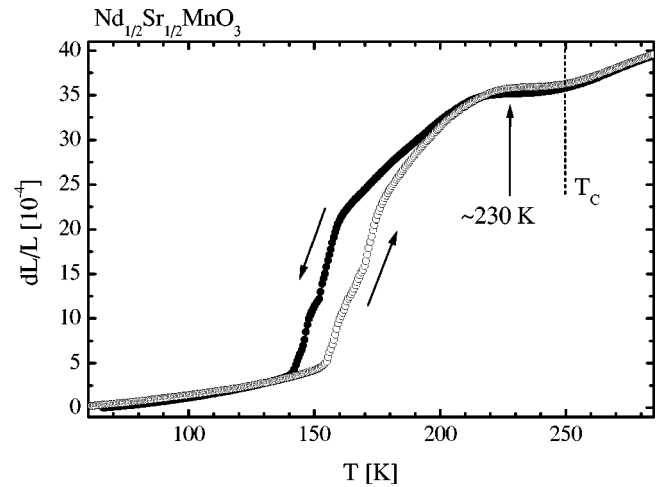

FIG. 4. Temperature hysteresis of the macroscopic length changes dL/L in zero field. dL/L shows a similar hysteretic behavior as the magnetization measurement displayed in Fig. 3.

teresis extends up to 230 K and, second, the temperature dependence between T_{CO} and T_C deviates considerably from that expected for a simple ferromagnet. More specifically, the magnetization starts to decrease already around 200 K upon cooling, suggesting the development of antiferromagnetic correlations. Note that we also observe an analogous feature of suppressed magnetization in elevated magnetic fields around 4 T (Fig. 10), excluding effects due to magnetic domains. Furthermore, this observation is in agreement with recent neutron scattering experiments where the onset of A-type antiferromagnetic correlations at 200 K has been observed.[15] An unusual hysteretic behavior similar to that observed in the magnetization is also found in the macroscopic length changes dL/L shown in Fig. 4 (L: macroscopic sample length). In particular, dL/L also displays a nonsymmetric temperature hysteresis and, moreover, the onset of anomalous contributions can be observed around 230 K. As the dL/L measurement is a highly sensitive probe for the investigation of structural changes the comparison with the magnetization measurements shows that the onset of antiferromagnetic correlations in the FMM phase is connected to structural distortions.

The onset of orbital ordering in the FMM phase provides a natural explanation for the unusual behavior found in the M and dL/L measurements, but such a microscopic origin cannot be clarified from the macroscopic behavior. However, recent neutron scattering experiments performed by Kawano and co-workers[15] revealed the existence of almost two-dimensional magnetic fluctuations corresponding to the A-type antiferromagnetic ordering. Moreover, Kiryukhin *et al.*[14] investigated the same samples used in the present study utilizing x-ray scattering as a probe for structural fluctuations. Although the ferro-orbital ordering of the A-type antiferromagnetic phase does not lead to additional superstructure reflections due to a larger unit cell, the authors found indications for almost two-dimensional fluctuating structural domains of a second phase above T_{CO} and argued that these domains exhibit A-type orbital order. The two-dimensional character of the magnetic and structural correlations found in
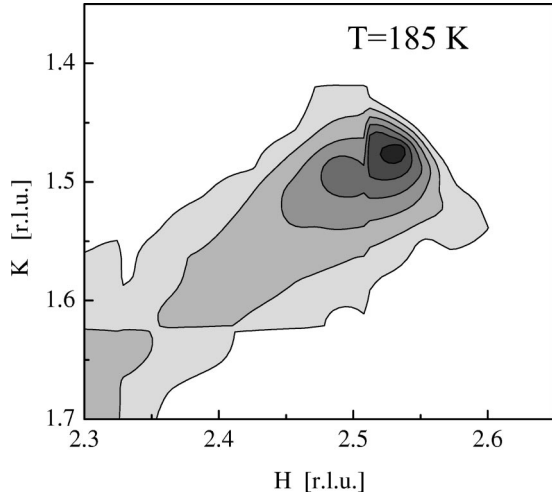
FIG. 5. Intensity distribution in the vicinity of the (220) reflection at $T = 185$ K. A broad peak centered at (2.5,1.5,0) can clearly be observed. The intensity around the (2.5,1.5,0) position merges into the strong anisotropic diffuse scattering around the (220) reflection.
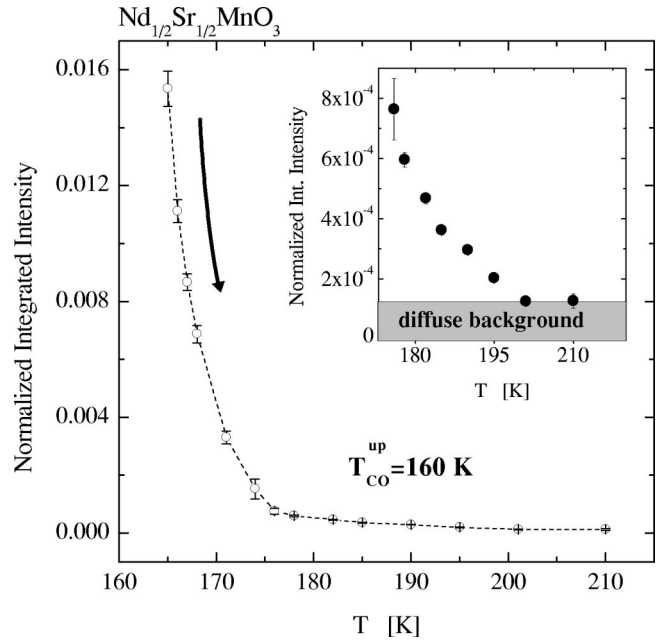

FIG. 6. Zero-field temperature dependence of the integrated intensity above T_{CO} taken at increasing temperature. The inset shows an enlarged view of the high-temperature regime above 180 K. Above 200 K the intensity of the (2,3/2,0) superstructure reflection merges into the diffuse background originating from the (220) Bragg reflection.

the two scattering experiments has been explained by the underlying A-type orbital order, which builds a two-dimensional orbital network of $d_{x^2-y^2}$ orbitals inside the ab planes.[1] Therefore, the results from the investigation of the macroscopic and microscopic properties can easily be understood in terms of short-range A-type orbital correlations in the FMM phase which couple to the magnetism as well as to the structure.

Next, we discuss the results of the hard x-ray scattering experiments. In Fig. 5 the intensity distribution in the vicinity of the orthorhombic (220) reflection is shown. A broad and anisotropic peak is observed centered around the (2.5,1.5,0) position, which merges into the strong anisotropic diffuse scattering around the (220) reflection. Note, that the intensity at the (2.5,1.5,0) position can be attributed to the (221) reflection of a different twin domain. These results are in agreement with the observations of Kiryukhin *et al.* mentioned above, indicating the presence of A-type orbital order. But moreover, we do also observe CE-type orbital correlations: Unlike the A-type orbital order, the CE-type orbital order gives rise to a larger unit cell, because its leads to a doubling along the b direction (Fig. 1). Therefore, this type of orbital order can be observed in a more direct way using x rays by investigating the corresponding additional superstructure reflections. In particular, we used hard x-ray scattering to investigate the temperature dependence of the (2,3/2,0) superstructure reflection above T_{CO}. As demonstrated in Fig. 6, intensity can be observed at the (2,3/2,0) position up to about 200 K upon heating. Above 200 K the intensity of the superstructure peak lies below a strong diffuse background centered at the (220) Bragg reflection, which can be attributed to the scattering from uncorrelated Jahn-Teller-polarons.[1,14,24,25] This is further illustrated in Fig. 7 where the temperature dependence of the radial and the l scan through the (2,3/2,0) reflection are compared. Note that the measurements have been performed with decreasing tem-

perature so that the CO/OO transition takes place at $T_{CO}^{down} = 150.5$ K. The radial scans in the left part of Fig. 7 consist of two contributions.

One very broad intensity distribution around $2\Theta \simeq -3.15°$ and another sharp and strongly temperature-dependent peak at $2\Theta \simeq -3°$ which can be identified as the (2,3/2,0) superstructure reflection. Obviously, the (2,3/2,0) reflection merges into the diffuse scattering, which limits the observation of the superstructure peak at high temperatures. But besides this, the radial scans reveal that the FWHM of the (2,3/2,0) reflection ($\Delta_{(2,3/2,0)}$) is almost constant and, moreover, comparable to the FWHM of the neighboring (220) Bragg peak ($\Delta_{(220)}$) which represents the experimental resolution. At the same time the l scans taken at the position of the sharp superstructure reflection show a pronounced broadening with increasing temperature. This anisotropic broadening of the (2,3/2,0) reflection is further illustrated in Fig. 8(a) which shows the temperature dependence of $\Delta_{(2,3/2,0)}/\Delta_{(220)}$ for the radial and l scans. The comparison clearly shows that the (2,3/2,0) superstructure reflection above T_{CO} is considerably broadened in the l direction, while it stays sharp in the radial direction. This indicates that above T_{CO} short-range CE-type orbital correlations exist predominantly in the ab plane whereas the correlations between the ab planes are weak. More specifically, our measurements show that on cooling the in-plane correlation length of the orbital ordering around 180 K is already about 500 Å, while the correlation length in the perpendicular direction is only about 80 Å. Another remarkable observation concerns the lattice constants of the short-range orbital-ordered areas which differ from those of the mean lattice.

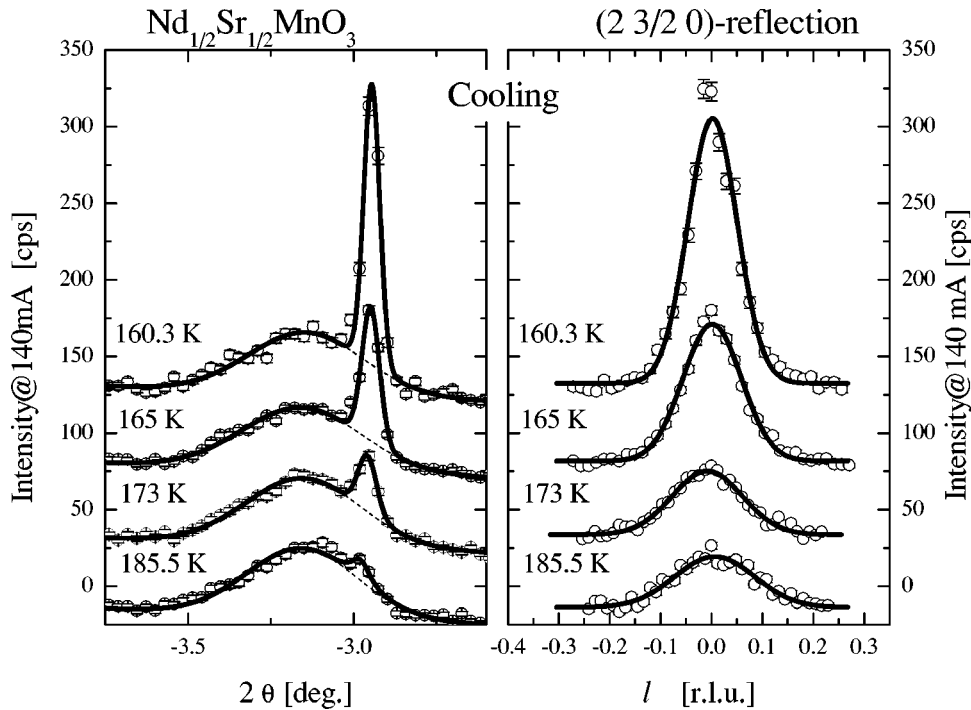This can be seen in Fig. 8(b) which shows the temperature

FIG. 7. Comparison of the temperature dependencies observed in the radial (left) and the l scan (right). Successive scans have been taken in zero field on cooling.

dependence of $\Delta d/d$, where d is lattice plane spacing corresponding to the (220) and (2,3/2,0) reflections, respectively. Approaching T_{CO} from below, $\Delta d/d$ for the (220) and (2,3/2,0) lattice planes display a rather similar behavior which is expected from the temperature dependence of the lattice parameters. At T_{CO} the lattice plane spacing corresponding to the (220) reflection changes drastically, due to the structural phase transition. The relative change $\Delta d/d \simeq -4.5 \times 10^{-3}$ agrees well with the changes of the lattice parameters reported in previous literature.[11] These changes of the mean lattice structure are not reflected by the lattice plane spacing corresponding to the (2,3/2,0) reflection. In particular, the lattice plane spacing corresponding to the (2,3/2,0) reflection shows the opposite behavior above T_{CO}, as it increases again to zero. This demonstrates that the periodicity

of the structural modulations decouples from the mean lattice structure approaching again its low-temperature value. It can be concluded that the lattice spacings in the short-range orbital-ordered areas differ from those of the mean lattice structure, thus being incommensurate. Incommensurate short-range charge and orbital order has also been observed in $Pr_{0.5}Ca_{0.5}MnO_3$ and $La_{0.5}Ca_{0.5}MnO_3$ using neutron and x-ray scattering techniques.[24,26,27]

To summarize so far, the above results obtained from the hard x-ray scattering experiments reveal the existence of short-ranged structural modulations between T_{CO} and 200 K. The corresponding correlation length is highly anisotropic; i.e., the correlation length in the ab plane is about 6 times larger than in the perpendicular direction. These short-range correlations above T_{CO} are incommensurate with the mean
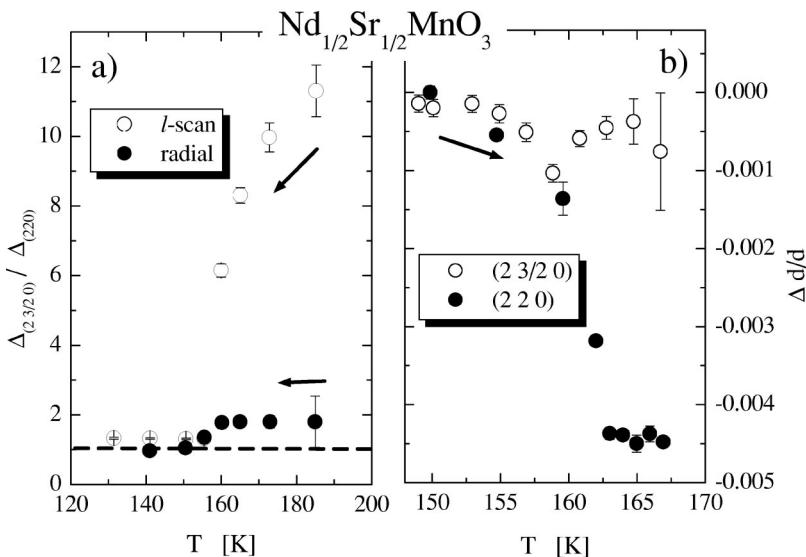

FIG. 8. (a) Comparison of the temperature dependencies of $\Delta_{(2,3/2,0)}/\Delta_{(220)}$ for the radial and l scans in zero magnetic field. (b) Comparison of the temperature dependencies of $\Delta d/d$ for the (220) and (2,3/2,0) reflections in zero field.
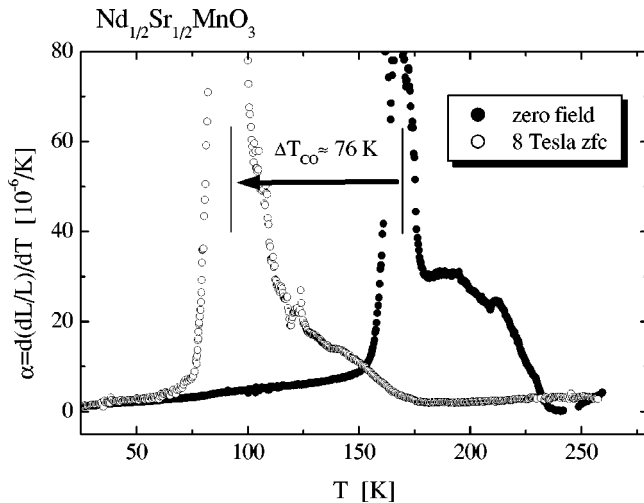
FIG. 9. Comparison of a field-cooled (FC) and a zero-field-cooled (ZFC) measurement of α taken at increasing temperature.
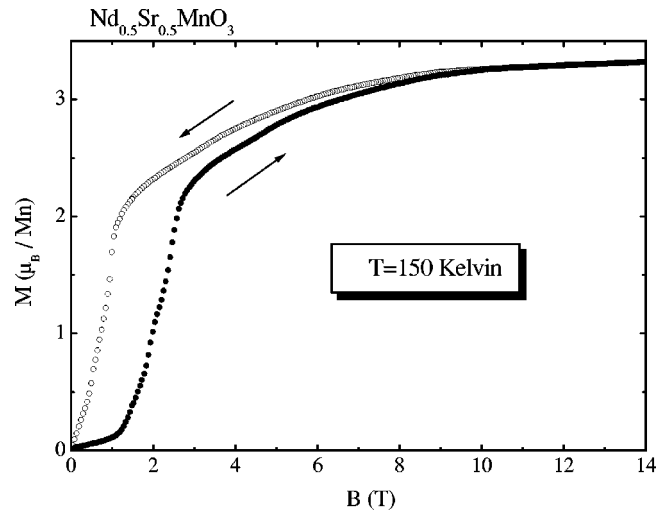

FIG. 10. Hysteresis loop of the macroscopic magnetization taken at $T = 150$ K$< T_{CO}$. The strong increase (decrease) of the magnetization with increasing (decreasing) field signals the phase transition between the CE and FMM phases.

lattice structure and, moreover, have lattice spacings similar to the CE phase below T_{CO}. Therefore, these results strongly indicate the presence of almost two-dimensional CE-type orbital-ordered areas between T_{CO} and 200 K in the ab plane which are weakly correlated along the c direction.

As the CE-type orbital ordering also takes place inside the ab planes building nearly one-dimensional zigzag chains (Fig. 1) along the b direction it is natural to assume that the planar character of the observed structural modulations is the result of the underlying CE-type orbital order. Furthermore, we mention, again, that the coexistence of the A, CE, and FMM phases above T_{CO} is in agreement with the fact that these phases are nearly degenerate in energy, which has been proved by experimental and theoretical investigations.[11,13,16,17]

Finally, we mention again that the development of A- and CE-type short-range orbital ordering in the FMM phase naturally explains the anomalous behavior observed between 230 K and T_{CO} in the magnetization and thermal expansion, since the orbital ordering couples to the magnetic exchange interactions as well as to the structure.

V. FIELD-DEPENDENT MEASUREMENTS

Next, we discuss the influence of applied magnetic fields on the CO/OO transition. Figure 9 compares two zero-field-cooled warming measurements[28] of the thermal expansion coefficient α which is the first temperature derivative of dL/L discussed in the previous section. The first measurement has been performed in zero field and the second one was done in an applied magnetic field of 8 T. Focusing on the zero-field measurement, the onset of anomalous contributions is observed around 230 K. These anomalous length changes are connected to the unusual hysteresis of dL/L shown in Fig. 4. The structural phase transition at T_{CO} is signaled by a pronounced anomaly in α around 160 K. This anomaly is shifted about 76 K in an external field of 8 T. But moreover, the anomalous contributions to α are also shifted to lower temperatures by a similar amount. This strongly

supports our conclusion that the anomalous length changes observed in the thermal expansion are directly connected to orbital ordering processes, because the A- and CE-type orbital ordering induces antiferromagnetic interactions which are destabilized in applied magnetic fields.

The destabilization of the long-range-ordered antiferromagnetic CE phase by the application of a magnetic field is shown in Fig. 10. In this figure a magnetization versus applied magnetic field curve taken at 150 K$< T_{CO}$ is shown. Starting from the zero-field-cooled state at $B = 0$ T the magnetization M below 1.2 T shows a typical antiferromagnetic behavior, i.e., a small magnetization which is proportional to the applied magnetic field. As the CO/OO transition is shifted to lower temperatures by the application of a magnetic field (see Fig. 9) the transition from the antiferromagnetic CE to the FMM phase is induced by further increasing the magnetic field strength. This field-induced phase transition is signaled by the strong increase of M between 1.2 and 3 T. However, the field dependence of M above 3 T deviates considerably from that expected for a ferromagnetic material. In particular, between 3 and 10 T M increases slowly and lies well below the saturation value of about $3.5\mu_B$/Mn. Furthermore, a pronounced field hysteresis is observed, manifesting once again the first-order character of the CO/OO transition. Note that in this field regime it is very unlikely that magnetic domains are responsible for the reduced magnetization M $< 3.5\mu_B$/Mn. Therefore, the field-dependent magnetization measurement strongly indicates the presence of antiferromagnetic correlations even at high magnetic fields within the ferromagnetic majority phase.

The destabilization of the long-range-ordered CE phase in applied magnetic fields is also demonstrated in Fig. 11, where the field dependence of the integrated intensity at the (2,7/2,0) position at 140 K is presented. The strong reduction of the integrated intensity with increasing field reflects the collapse of the long-range charge- and orbital-ordered CE phase. However, similar to the temperature-dependent stud-
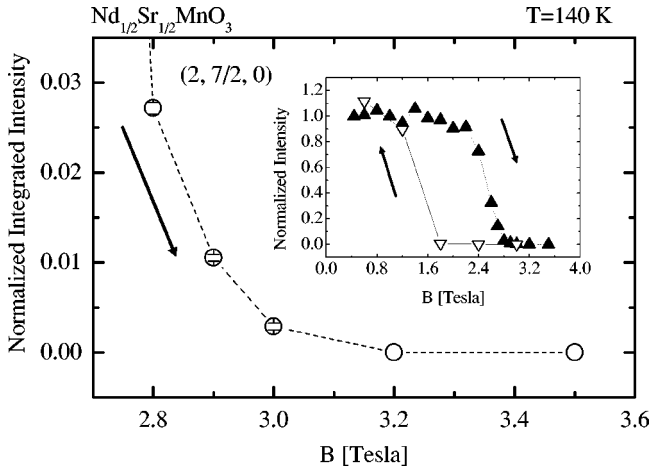
FIG. 11. Field dependence of the integrated intensity of the $(2,7/2,0)$ reflection taken at 140 K$<T_{CO}$ in the FMM phase. The inset displays the field hysteresis of the integrated intensity at the $(2,7/2,0)$ position.

ies, not all of the intensity vanishes above the critical field. Moreover, we again observe that the FWHM of the radial scan is nearly unchanged across the phase transition as demonstrated in Fig. 12. Obviously, the integrated intensity of the $(2,7/2,0)$ reflection is reduced by a factor of 140, while the FWHM stays almost constant across the field-induced phase transition.[29] Furthermore, it can be seen in Fig. 12 that the position of the $(2,7/2,0)$ reflection is also almost unchanged across the phase transition; i.e., the periodicity of the structural modulation does not change. Unfortunately, we could not observe the broadening in the l direction due to experimental restrictions.[30] However, the results strongly indicate that the same short-range orbital ordering phenomenon which has also been observed above T_{CO} in zero field takes

place above the critical field. Indeed, the ferromagnetic order in the FMM phase produces considerable internal fields which act in a similar way as applied magnetic fields.

The field-dependent measurements of α, M, and the $(2,7/2,0)$ reflection strongly indicate the existence of antiferromagnetic correlations in the field-induced FMM phase which are connected to structural modulations. Again, the presence of short-range A- and CE-type orbital correlations in the FMM phase provides a natural explanation for the experimental observations given above.

VI. SUMMARY AND CONCLUSION

We have presented magnetization, thermal expansion, and hard x-ray scattering studies on Nd$_{1/2}$Sr$_{1/2}$MnO$_3$ as a function of temperature and magnetic field. The hard x-ray studies indicate the presence of incommensurate and highly anisotropic CE-type short-range orbital correlations in the FMM phase which can naturally explain the anomalous features found in the magnetization and thermal expansion measurements: The onset of A- and CE-type orbital ordering inside the ab planes leads to a reduction of the macroscopic sample length in the c direction which is observed in the thermal expansion.[31] Furthermore, the orbital correlations induce antiferromagnetic interactions in agreement with the magnetization measurements. As the presence of A-type correlations has already been reported in the previous literature[14,15] it is very likely that between T_{CO} and 200 K three phases coexist: namely, the A-, CE-type, and FMM phases. The coexistence of three phases is further indicated by numerous experimental and theoretical investigations which show that these three phases are nearly degenerate in energy.[13,16] We conclude that at T_{CO} the long-range charge- and orbital-ordered CE phase collapses and phase segregation occurs between T_{CO} and 230 K. In this temperature regime short-range A- and CE-
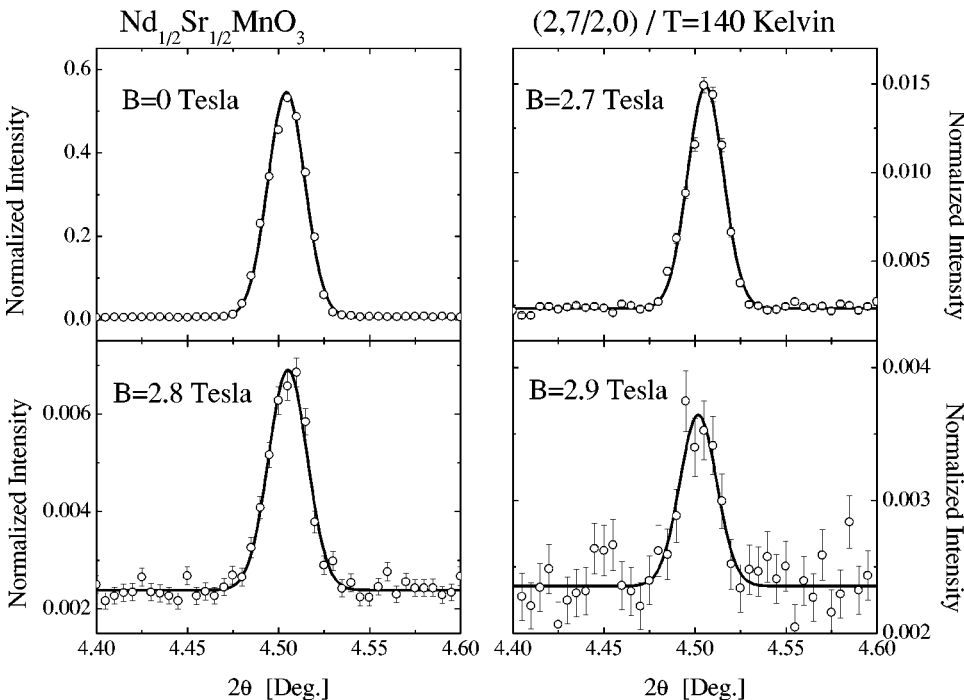

FIG. 12. Field dependence of the radial scans taken at the $(2,7/2,0)$ position at 140 K. The width and position of the superstructure reflection are nearly field independent. The measurements have been performed with increasing field.

type orbital correlations persist in the FMM phase. It is important to note that the large-scale phase separation indicated by the hard x-ray results is in agreement with the fact that the three coexisting phases have similar charge carrier concentrations. In this case long-range Coloumb interactions do not prevent the large-scale phase segregation.[18] Finally, we demonstrated that long-range CE-type orbital ordering collapses at a critical magnetic field. Above this critical field the short-range CE-type orbital correlations exist and are continuously reduced with further increasing field. We argue that short-range orbital order can persist in the ferromagnetic metallic phase or in applied magnetic fields by strongly reducing the correlations between successive *ab* planes and thereby re-

ducing the antiferromagnetic interactions between them. The results given above show that phase segregation and percolative effects are of fundamental importance for the CMR effect of this compound.

[1] Y. Tokura and N. Nagaosa, Science **288**, 462 (2000).

[2] S. Uhlenbruck *et al.*, Phys. Rev. Lett. **82**, 185 (1999).

[3] A. Millis, Nature (London) **392**, 147 (1998).

[4] E. O. Wollan and W. C. Koehler, Phys. Rev. **100**, 545 (1955).

[5] Y. Tomioka, A. Asamitsu, Y. Moritomo, H. Kuwahara, and Y. Tokura, Phys. Rev. Lett. **74**, 5108 (1995).

[6] Z. Jirác S. Krupika, Z. Simsa, M. Dlouhá, and S. Vratislav, J. Magn. Magn. Mater. **53**, 153 (1985).

[7] P. Radaelli, P. E. Cox, M. Marezio, and S.-W. Choeng, Phys. Rev. Lett. **75**, 4488 (1995).

[8] K. Nakamura, T. Arima, A. Nakazawa, N. Wakabayashi, and Y. Murakami, Phys. Rev. B **60**, 2425 (1999).

[9] K. Kuwahara, Y. Tomioka, A. Asamitsu, Y. Moritomo, and Y. Tokura, Science **270**, 961 (1995).

[10] B. Sternlieb, J. P. Hill, U. C. Wildgruber, G. M. Luke, B. Nachumi, Y. Moritomo, and Y. Tokura, Phys. Rev. Lett. **76**, 2169 (1996).

[11] R. Kajimoto, H. Yoshizawa, H. Kawano, H. Kuwahara, Y. Tokura, and K. O. M. Ohashi, Phys. Rev. B **60**, 9506 (1999).

[12] J. van den Brink, G. Khaliullin, and D. Khomskii, Phys. Rev. Lett. **83**, 5118 (1999).

[13] T. Fujiwara and M. Korotin, Phys. Rev. B **59**, 9903 (1999).

[14] V. Kiryukhin, B. G. Kim, T. Katsufuji, J. P. Hill, and S.-W. Cheong, Phys. Rev. B **63**, 144406 (2001).

[15] H. Kawano, R. Kajimoto, H. Yoshizawa, Y. Tomioka, K. Kuwahara, and Y. Tokura (unpublished).

[16] C. Ritter, R. Mahendiran, M. Ibarra, L. Morellon, A. Maignan, B. Raveau, and C. Rao, Phys. Rev. B **61**, R9229 (2000).

[17] P. Woodward, D. Cox, T. Vogt, C. Rao, and A. Cheetham, Chem. Mater. **11**, 3528 (1999).

[18] A. Moreo, S. Yunoki, and E. Dagotto, Science **283**, 2034 (1999).

[19] M. Uehara, S. Mori, C. H. Chen, and S.-W. Cheong, Nature (London) **399**, 560 (1999).

[20] Z. Popovic and S. Satpathy, Phys. Rev. Lett. **88**, 197201 (2002).

[21] T. Mutou and H. Kontani, Phys. Rev. Lett. **86**, 2479 (2001).

[22] S. Foner, Rev. Sci. Instrum. **27**, 548 (1956).

[23] T. Lorenz, U. Ammerahl, T. Auweiler, B. Büchner, A. Revcolevschi, and G. Dhalenne, Phys. Rev. B **55**, 5914 (1997).

[24] S. Shimomura, T. Tonegawa, K. Tajima, N. Wakabayashi, N. Ikeda, T. Shobu, Y. Noda, Y. Tomioka, and Y. Tokura, Phys. Rev. B **62**, 3875 (2000).

[25] S. Shimomura, N. Wakabayashi, H. Kuwahara, and Y. Tokura, Phys. Rev. Lett. **83**, 4389 (1999).

[26] R. Kajimoto, H. Yoshizawa, Y. Tomioka, and Y. Tokura, Phys. Rev. B **63**, 212407 (2001).

[27] Q. Huang, J. W. Lynn, R. W. Erwin, A. Santoro, D. C. Dender, V. N. Smolyaninova, K. Ghosh, and R. L. Greene, Phys. Rev. B **61**, 8895 (2000).

[28] This means that the sample has been cooled down in zero field before the measurement was performed with increasing temperature.

[29] Note that the diffuse background depends strongly on the position in reciprocal space (Refs. 25 and 24).

[30] The *l* direction was perpendicular to the scattering plane. Therefore, the experimental resolution in this direction was poor.

[31] As the thermal expansion shows a steep decrease of the sample length at T_{CO} upon cooling, this measurement mainly reflects changes of the *c* axis.